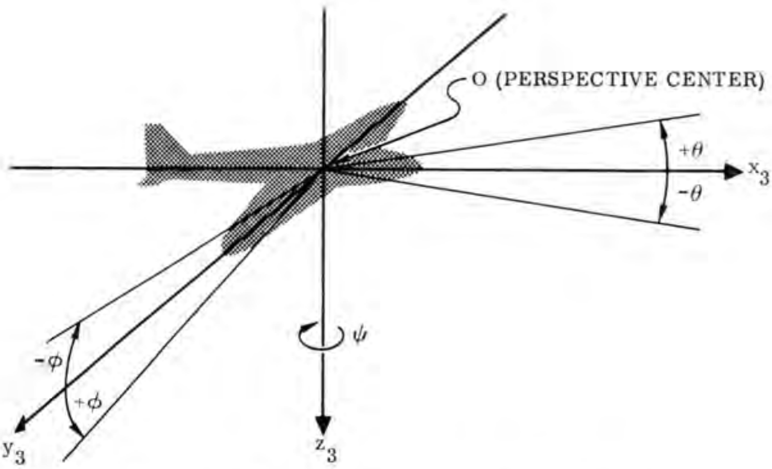

FIG. 1. Aircraft coordinate system. (See page 1160.)

DR. J. I. GIMLETT*
Hycon Company
Monrovia, Calif. 91016

Image Smears

Computer programs help in the analysis of motion blur due to velocity, roll, pitch, and yaw for frame and pan photos

INTRODUCTION

TRANSLATIONAL and rotational aircraft motions lead to image smears in aerial photography. The effect of forward motion can be minimized by a forward motion compensation (FMC) system, which involves moving the lens, film, or platen, or rocking (panning) the camera during the exposure. Stabilized platforms are often utilized as camera mounts to reduce smear caused by the roll, pitch, and yaw (RPY) motions of the vehicle. The interaction between FMC system, platform instability, and aircraft translation (all for various camera and vehicle attitudes) creates a formidable problem for manual calculations. The complete solution of the image motion problem is, however, a routine computer application.

In order to describe completely the complex camera-aircraft-ground geometries encountered in a reconnaissance environment it was found necessary to define six angles instead of the customary three. Three angles are used to specify vehicle orientation with respect to the ground and three to relate camera and vehicle. All six must be permitted to vary with time. The time variations of the first set of three angles are the familiar RPY motions. Variations of the second set are possible FMC motions. The two horizontal components of vehicle motion are usually specified by the air-to-ground speed and the angle relating direction of travel to the ground coordinate system.

No published analyses, known to the author, completely cover the six angular coordinates and their time derivatives. However, several of the published approaches would, with a few modifications, be highly applicable (Hallert, 1960; Kawachi, 1965a,

* Presented at the Semi-Annual Convention of the American Society of Photogrammetry, Los Angeles, Calif., September 1966.

and 1965b; Manual of Photogrammetry, 1966).

The selected approach is as follows. The six angular coordinates are used to specify six rotational transformations, each characterized by its own 3×3 matrix. This property of *separability*, which leads to analytical and programming simplicity, requires that the angles be defined in two sets of three Euler angles. These matrics are never multiplied out formally; the computer performs all matrix multiplications. Image and ground (object) are connected via conventional projective transformations. No formal differentiation of the projective equations is attempted to determine the effects of motion. Rather, the components of image smear are found directly as the finite differences between the image coordinates corresponding to the positions of an object point at the beginning and at the end of the exposure.

Two of the other-than-computational advantages of this approach are: (1) the assumption of linear motion is unnecessary, as the method can be easily programmed to cover motions with any arbitrary, but specified, time variations; (2) ground coordinates, corresponding to grid points on the positive, are computed as a matter of course, hence are available for use in point-by-point rectifiers. Thus, panoramic and focal-plane-shuttered cameras with calibrated FMC systems and curtain velocities retain their full metric potential.

Two computer routines, based on this approach, were programmed in Fortran for the CDC 3600. Program IMS002 computes: (1) ground coordinates corresponding to a rectangular grid over the entire format; (2) image smear components for any, or all, of four motions (forward motion, RPY) at each point of the grid; and (3) corresponding three-bar resolutions and AWAR (Area Weighted Average Resolution). It encompasses framing, mirror-framing, and panoramic cameras; intralens or focal plane shutters; and moving lens-film, rocking, graded, and bimodal FMC systems.

The RPY rates and V/H-sensor error are essentially satistical quantities. Program MCIMS deterministically solves the image motion problem by means of a Monte Carlo simulation of the concomitant probabilistic problem. The RPY and V/H-error (including both the sensor error and the effect of the topography) distributions are sampled to determine the operating conditions for any one case. The image smears and corresponding AWARs for 100 such cases are calculated and the performance S-curve derived. Many of the subroutines are shared by the two programs.

ABSTRACT: *The salient features of a generalized smear (motion blur) analysis and some computer results relate to image resolution. The analysis utilizes conventional coordinate and projective transformations, except that all matrix multiplications and differentiations are performed on the computer rather than formally. Linearity need not be assumed. Also, six angular coordinates (two sets of Euler angles) are specified instead of the customary three. Program IMS002, used primarily in camera design, prints out: (1) ground coordinates corresponding to the points of a rectangular grid in the negative, (2) image smear components, due to the vehicular roll, pitch, yaw, and forward motions, at each grid point, and (3) corresponding three-bar resolutions. IMS002 encompasses framing, mirror-framing, and panoramic cameras equipped with intra-lens or focal plane shutters. Moving lens-film, rocking, graded, and bimodal (forward-looking panoramic) forward motion compensation methods are explicitly covered. Program MCIMS uses Monte Carlo simulation to predict system performance.*

ANALYSIS FOR SMEAR PROGRAM

COORDINATE SYSTEMS

There are actually four right-handed coordinate systems all with origin at the perspective center, of importance to this analysis. The Cartesian coordinate system (x_p, y_p, $z_0 = f$), which serves as the point of departure for all calculations, describes the positive image plane with $0, 0, f$ being the principal point in the positive image. The second system (x_f, y_f, $z_0=f$), which describes the camera format, coincides with the first in all framing cameras which do not have moving lens, film, or platen FMC mechanisms. In panoramic cameras the two systems are related, neglecting FMC for the nonce, by a projective transformation of the form

$$x_f = x_p \sec (y_p/f)$$
$$y_f = f \tan (y_p/f) \qquad (1)$$

where f is the focal length. For framing cameras in which the film is moved in the x_p-direction during the exposure the two systems are related by

$$x_f = x_p - (V/H)F(t)$$
$$y_f = y_p \qquad (2)$$

where V/H is the measured or predicted (as opposed to true) velocity-altitude ratio and $F(t)$ is a function of time (linear, for constant FMC film velocity).

The aircraft system (x_3, y_3, z_3), as shown in Figure 1, page 1158, agrees with more or less conventional aeronautical engineering practice (see for example Perkins and Hage, 1949); i.e. x_3 is in the direction of flight, y_3 is perpendicular to x_3 and to the plane of symmetry, positive in the direction of the right wing, and z_3 is positive downward. The ground system (X, Y, H) is fixed such that (0, 0, H) is the nadir point. The directions of X and Y can be specified to any ground coordinate system. However, lacking information to the contrary, X is selected as the direction of flight. Similarly the x_f-direction is chosen to be the camera coordinate most closely corresponding to the direction of flight.

The general transformation, the result of the six angular rotations, relates the x_f, y_f, z_0 and X, Y, Z coordinate systems with the x_3, y_3, z_3 serving as one of the intermediates. All calculations are performed in centimeters. (Output in kilometers and microns can then be handled by simple P Fortran format specification.)

ROTATIONS

The two sets of Euler angles are shown in Figures 1 and 2. The angles are self-explanatory except for ψ_s, the swing setting, and ψ the yaw angle. The angle ψ_s can be considered the angle between the fiducial x_f-axis and the intended flight path in the image plane (i.e. neglecting aircraft RPY). As such, it must depend on the particular aircraft-camera geometry under consideration. For example, in a rolled frame (side-looking) taken with a mirror-type (*elephant nose*) camera,

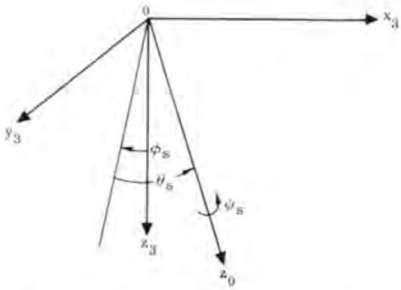

FIG. 2. Camera-aircraft orientation.

$$\psi_s = \psi_0 + \phi_s \qquad (3)$$

where ψ_0 depends on the method of mounting the camera to the air-frame. To avoid skewing, the format is automatically rotated in certain Hycon mirror cameras so that $\psi_0 = -\phi_s$. Ordinarily ψ_s is set to zero, i.e. the x_f-axis coincides with the aircraft x_3-axis.

The yaw angle ψ, which corresponds closely to the photogrammetric crab angle η, should probably be written

$$\psi = \eta + \psi' \qquad (4)$$

where ψ' is the angle between the flight path and the ground reference X, which might be the northing in a U.T.M. coordinate system, for example.

Following the indicated sign conventions the six orthogonal rotation matrices are given as follows:

$$M_1 = \begin{bmatrix} \cos\psi_s & \sin\psi_s & 0 \\ -\sin\psi_s & \cos\psi_s & 0 \\ 0 & 0 & 1 \end{bmatrix}$$
$$M_2 = \begin{bmatrix} \cos\theta_s & 0 & \sin\theta_s \\ 0 & 1 & 0 \\ -\sin\theta_s & 0 & \cos\theta_s \end{bmatrix}$$
$$M_3 = \begin{bmatrix} 1 & 0 & 0 \\ 0 & \cos\phi_s & \sin\phi_s \\ 0 & -\sin\phi_s & \cos\phi_s \end{bmatrix}$$
$$M_4 = \begin{bmatrix} 1 & 0 & 0 \\ 0 & \cos\phi & -\sin\phi \\ 0 & \sin\phi & \cos\phi \end{bmatrix}$$
$$M_5 = \begin{bmatrix} \cos\theta & 0 & \sin\theta \\ 0 & 1 & 0 \\ -\sin\theta & 0 & \cos\theta \end{bmatrix}$$
$$M_6 = \begin{bmatrix} \cos\psi & -\sin\psi & 0 \\ \sin\psi & \cos\psi & 0 \\ 0 & 0 & 1 \end{bmatrix}. \qquad (5)$$

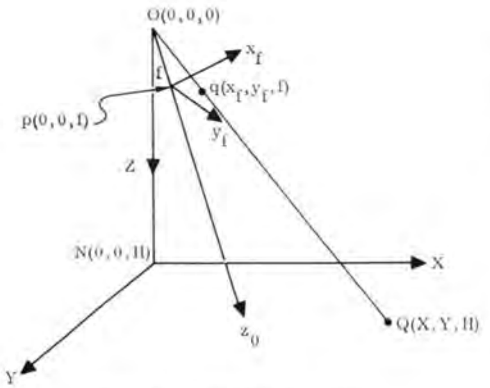

FIG. 3. Projective geometry.

Indicating the time dependence explicitly, the combined image-to-object-space transformation can be written as

$$\begin{bmatrix} X \\ Y \\ Z \end{bmatrix} = M(t)\begin{bmatrix} x_f \\ y_f \\ z_0 \end{bmatrix} \tag{6}$$

where

$$M(t) = M_6(\psi)M_5(\theta)M_4(\phi)M_3(\phi_s)M_2(\theta_s)M_1(\psi_s). \tag{7}$$

The inverse, object-to-image-space, transformation is given by

$$\begin{bmatrix} x_f \\ y_f \\ z_0 \end{bmatrix} = M_1^{-1}M_2^{-1}M_3^{-1}M_4^{-1}M_5^{-1}M_6^{-1}\begin{bmatrix} X \\ Y \\ Z \end{bmatrix}$$

$$= M^{-1}(t)\begin{bmatrix} X \\ Y \\ Z \end{bmatrix}. \tag{8}$$

It must be remembered that in any Euler angle transformation the order of the rotations is fixed. If the aircraft is equipped with an inertial platform, the sequence of rotations indicated in Equation 6 assumes that the outer indicator bail of the vertical reference gyro measures pitch θ and the inner, roll ϕ. The sequence of camera-pointing rotations was selected so as to be in accord with design practice in certain mirror cameras where side-looking frames are obtained by rotating the head containing the mirror about the longitudinal camera axis (the aircraft x_3-axis) through the angle ϕ_s. The camera is then aimed fore-and-aft by rocking the mirror through an angle equal to one-half θ_s about the new axis.

The sequence would have to be changed for other conditions. However, any camera-aircraft or aircraft-ground orientation can be achieved with the angles and order of rotations herein specified. Also, for small rotations, the order is immaterial.

PROJECTIVE TRANSFORMATION

The relationship between points in the positive image plane and points on the ground plane is established by the conventional (Hallert, 1960) projective transformation. (See Figure 3). The air-to-ground projective transformation can be written as

$$\frac{X}{H} = \frac{M_{11}x_f + M_{12}y_f + M_{13}f}{M_{31}x_f + M_{32}y_f + M_{33}f}$$

$$\frac{Y}{H} = \frac{M_{21}x_f + M_{22}y_f + M_{23}f}{M_{31}x_f + M_{32}y_f + M_{33}f}. \tag{9}$$

The inverse, ground-to-air, projective transformation is then

$$\frac{x_f}{f} = \frac{M_{11}^{-1}X + M_{12}^{-1}Y + M_{13}^{-1}H}{M_{31}^{-1}X + M_{32}^{-1}Y + M_{33}^{-1}H}$$

$$\frac{y_f}{f} = \frac{M_{21}^{-1}X + M_{22}^{-1}Y + M_{23}^{-1}H}{M_{31}^{-1}X + M_{32}^{-1}Y + M_{33}^{-1}H}. \tag{10}$$

TIMING

In order to describe motions it is obviously necessary to establish a time scale. As a first step we define T_1 to be the time at which exposure at an arbitrary point x_f, y_f begins, and T_2 the time at which it ends. Then for all points and cameras the exposure time T_E will be given by

$$T_E = T_2 - T_1, \tag{11}$$

i.e. assuming rectangular shutter pulses. The time at the instant of exposure, i.e. when the center of a focal plane shutter slit crosses x_f, y_f is the time TI. The origin of the time scale $TI=0$ is specified as the instant when the center of the slit crosses the principal point $x_f=y_f=0$. With this definition we can write for all cameras

$$T_1 = TI - T_E/2$$

$$T_2 = TI + T_E/2, \tag{12}$$

where TI obviously depends on the velocity of the shutter curtain, its direction of travel, and on x_f, y_f. Values of TI for various shutters are tabulated in Table 1. Focal-plane-shutter curtain velocity is given by v_s, and the panoramic angular scan velocity by ω_s. Notice ω_s and v_s are both signed constants as the shutter curtains can move in either direction. In fact in some cameras the curtain alternates in its direction of travel.

Moving-film FMC systems in focal-plane cameras complicate the analysis and the programming. The initial step in all calcula-

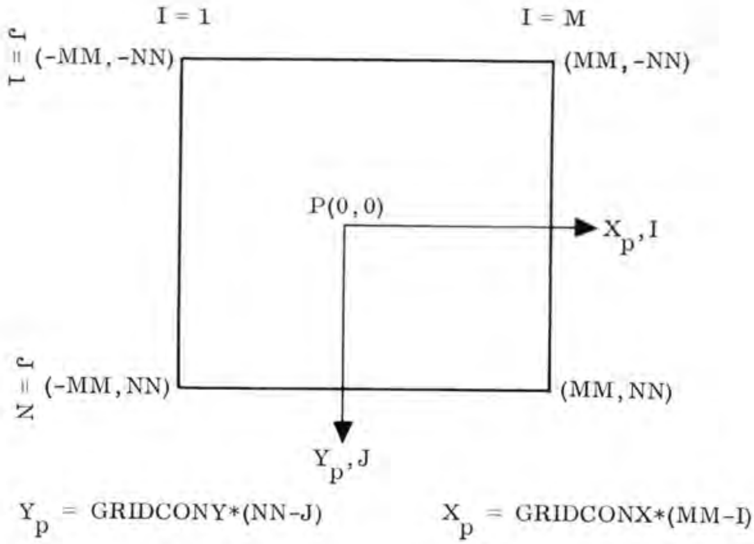

FIG. 4. Positive coordinate system.

tions is the establishment of a rectangular (GRIDCONX by GRIDCONY) grid x_p, y_p in the positive, as per Figure 4. In order to find the camera coordinates x_f, y_f corresponding to x_p, y_p in cameras with moving film systems, an iteration procedure is followed. As a complex example, let us consider a forward-looking panoramic camera which utilizes bimodal FMC, e.g. the film is moved in the y_p-direction while the lens translates in the x_p.

An initial estimate A_0 for the scan angle A can be obtained from

$$A_0 = y_p/f. \tag{13}$$

The iterative relationship for the n-th estimate is

$$A_n = A_0 - C \sin^2 (A_{n-1}), \tag{14}$$

where the constant C is given by

$$C = -1/2 \frac{V}{H\omega_s} \cos\theta_s \sin\theta_s. \tag{15}$$

It was found that sufficient accuracy could be obtained in only three iterations. For this case the complete set of equations for determining the time TI and x_f, y_f becomes

$$TI = \frac{A_3}{\omega_s}$$
$$y_f = f \tan A_3$$
$$x_f = \left(x_p - \frac{fV}{\omega_s H} \cos^2\theta_s \sin A_3\right) \sec A_3. \tag{16}$$

Similar iterative procedures are used for focal-plane framing cameras equipped with moving-film FMC systems.

TRANSLATIONS

Equation 9 can be used in the form

$$\frac{X}{H} = \frac{M_{11}(TI)x_f + M_{12}(TI)y_f + M_{13}(TI)f}{M_{31}(TI)x_f + M_{32}(TI)y_f + M_{33}(TI)f}$$
$$\frac{Y}{H} = \frac{M_{21}(TI)x_f + M_{22}(TI)y_f + M_{23}(TI)f}{M_{31}(TI)x_f + M_{32}(TI)y_f + M_{33}(TI)f} \tag{17}$$

to find the ground coordinates corresponding to the point x_f, y_f, which was exposed at time TI. Ground point X, Y, then, corresponds to the smear (point, if no image motion) centered (linearity assumed) at x_f, y_f or x_p y_p. The array of ground points X, Y corresponding to the positive grid points x_p, y_p is a portion of the output of program IMS002. A plot (printer in the case of framing cameras, Calcomp for panoramic cameras) of the ground grid is available as an option. The print-out and plot are especially useful for panoramic photography.

To find the image coordinates of the ends of a smear in the positive systems x_2, y_2 and x_1, y_1, it is first necessary to determine the corresponding ground coordinates X_2, Y_2

TABLE I. TIMING

Shutter	TI
Intralens	0
Focal Plane	
Curtain moves in x_f-direction	x_f/v_s
Curtain moves in y_f-direction	y_f/v_s
Panoramic	$y_f/f\omega_s$

and X_1, Y_1, respectively. This can be done by the translational transformation

$$X_k = X + (-1)^k V_x \cdot T_E/2$$
$$Y_k = Y + (-1)^k V_y \cdot T_E/2, \qquad k = 1, 2 \quad (18)$$

where V_x and V_y are the aircraft velocity components. Obviously a similar transformation could easily be applied to H, for example for moonshot photography. The ground-to-air projective transformation (Equation 10) is now applied in the form

$$\frac{x_k}{f} = \frac{M_{11}^{-1}(T_k)X_k + M_{12}^{-1}(T_k)Y_k + M_{13}^{-1}(T_k)H}{M_{31}^{-1}(T_k)X_k + M_{32}^{-1}(T_k)Y_k + M_{33}^{-1}(T_k)H}$$
$$\frac{y_k}{f} = \frac{M_{21}^{-1}(T_k)X_k + M_{22}^{-1}(T_k)Y_k + M_{23}^{-1}(T_k)H}{M_{31}^{-1}(T_k)X_k + M_{32}^{-1}(T_k)Y_k + M_{33}^{-1}(T_k)H},$$
$$k = 1, 2. \quad (19)$$

The x and y smear components, s_x and s_y, are then simply found from

$$s_x = x_2 - x_1 + x_{ft}$$
$$s_y = y_2 - y_1 + y_{ft} \qquad (20)$$

where the x_{ft} and y_{ft} are the distances the film (lens or platen) is moved during the exposure time by the FMC system. The total smear s, again considering the image motion to be linear,

$$s = (s_x^2 + s_y^2)^{1/2} \qquad (21)$$

can be used in resolution calculations. The *rms* smear over the format is also computed.

RESOLUTION

The total resolution R_{ij} at the ith, jth point in the positive is defined in this program as

$$R_{ij} = \frac{R_{0ij}}{1 + sR_{0ij}} \qquad (22)$$

where R_{0ij} is the static (lens-film) resolution at the point. Program options include computing R_{0ij} as the geometric mean of measured radial and tangential resolutions, or from an assumed *cos*²-falloff from the principal point. Also, it can be considered a constant over the format.

The convolution in Equation 22 should not be considered rigorous. It does, however, offer the following advantages: (1) it seems to agree with empirical results for low-contrast targets; (2) it is simpler to compute than some of the $R^{-1.8}$-type formulas; and (3) it is very reproducible and objective. An AWAR value equal to the average R_{ij} over the format is calculated. Again, this AWAR must not be considered equivalent to one measured according to Mil. Spec. 150A. It is, however, indicative and useful.

SMEAR PROGRAM IMS002

Program IMS002, as it currently stands, consists of the main calling program, eighteen subroutines, and two functions. The most recent changes involve additions to the plotting capability (smears can be represented as vectors on a Calcomp plot), and to subroutine RESOL1, which convolves image smear with static resolution. A portion of the output for a trial case is shown in Figures 5 to 8.

Figure 5 is a print-out of the pertinent camera data plus the computed ground coordinates and is entirely self-explanatory. The particular case is for a mirror camera, utilizing rocking FMC, in which the platen is automatically rotated through the side oblique angle, ϕ_s, to avoid skewing the format. The listed ground coordinates (in kilometers) are for the object points corresponding to the image points at the four corners, at the

```
IMAGE MOTION STUDY

ASP PAPER

   FORMAT 10.00 X 10.00 CM     FL=60.960 CM

   FORWARD   OBLIQUE   SWING    PITCH  ROLL  YAW
   POINTING  POINTING  SETTING                        ANGLES IN DEGREES
     0.0       45.0     -45.0    0.0    0.0   0.0

V= 770 FT/SEC    H= 70000 FT    TRUE V/H=0.0110 R/SEC
IMAGE SMEARS ARE COMPUTED ON A 1.000 BY 1.000 CM GRID.
FOCAL PLANE SHUTTER CURTAIN TRAVELS IN -Y-DIRECTION AT 203.20 CM/SEC
ROCKING FMC

GROUND COORDINATES IN KILOMETERS FOR A 5.000 BY 5.000 CM GRID IN THE NEGATIVE.

     -2.288     -0.000      2.287    X
     18.101     18.101     18.101    Y

     -2.475      0.000      2.475
     21.336     21.336     21.336

     -2.697     -0.001      2.695
     25.149     25.149     25.149
```

FIG. 5. Camera data—ground coordinates.

IMC IMAGE SMEAR IN MICRONS FOR NO V/H SENSOR ERROR, EXPOSURE TIME-0.0040 SEC.

-1.4	-1.5	-1.5	-1.5	-1.6	-1.6	-1.6	-1.5	-1.5	-1.5	-1.4	DX
0.1	0.1	0.1	0.1	0.0	-0.0	-0.0	-0.1	-0.1	-0.1	-0.1	DY
-1.1	-1.2	-1.2	-1.2	-1.2	-1.2	-1.2	-1.2	-1.2	-1.2	-1.1	
0.1	0.1	0.1	0.0	0.0	-0.0	-0.0	-0.0	-0.1	-0.1	-0.1	
-0.8	-0.9	-0.9	-0.9	-0.9	-0.9	-0.9	-0.9	-0.9	-0.9	-0.8	
0.1	0.1	0.0	0.0	0.0	-0.0	-0.0	-0.0	-0.0	-0.1	-0.1	
-0.5	-0.5	-0.6	-0.6	-0.6	-0.6	-0.6	-0.6	-0.6	-0.5	-0.5	
0.1	0.0	0.0	0.0	0.0	-0.0	-0.0	-0.0	-0.0	-0.0	-0.1	
-0.2	-0.2	-0.3	-0.3	-0.3	-0.3	-0.3	-0.3	-0.3	-0.2	-0.2	
0.0	0.0	0.0	0.0	0.0	-0.0	-0.0	-0.0	-0.0	-0.0	-0.0	
0.1	0.1	0.0	0.0	0.0	0.0	0.0	0.0	0.0	0.1	0.1	→ X_p
0.0	0.0	0.0	0.0	0.0	0.0	0.0	0.0	0.0	0.0	0.0	
0.4	0.4	0.4	0.3	0.3	0.3	0.3	0.3	0.4	0.4	0.4	
-0.0	-0.0	-0.0	-0.0	-0.0	-0.0	0.0	0.0	0.0	0.0	0.0	
0.8	0.7	0.7	0.6	0.6	0.6	0.6	0.6	0.7	0.7	0.7	
-0.1	-0.0	-0.0	-0.0	-0.0	-0.0	0.0	0.0	0.0	0.0	0.1	
1.1	1.0	1.0	1.0	0.9	0.9	0.9	1.0	1.0	1.0	1.1	
-0.1	-0.1	-0.0	-0.0	-0.0	-0.0	0.0	0.0	0.0	0.1	0.1	
1.4	1.3	1.3	1.3	1.2	1.2	1.2	1.3	1.3	1.3	1.4	
-0.1	-0.1	-0.1	-0.0	-0.0	-0.0	0.0	0.0	0.1	0.1	0.1	
1.7	1.6	1.6	1.6	1.6	1.6	1.6	1.6	1.6	1.6	1.7	
-0.1	-0.1	-0.1	-0.1	-0.0	-0.0	0.0	0.1	0.1	0.1	0.1	

RMS SMEAR= 1.0 MICRONS.

↓ Y_p

FIG. 6. Image smears due to forward motion.

centers of the sides, and at the center (principal point) of the 10×10 centimeter grid.

Figure 6 is a plot of the smears due to imperfect FMC. It should be noted, that because rocking produces hyperbolic image paths, perfect FMC can never be achieved with a rocking system. However, the superiority of rocking FMC over no FMC is indicated by an AWAR of 92 versus 35 lines/mm. Table II shows the effect of V/H error. Notice that slight under-compensation produces a smaller *rms*-smear. The resolution array corresponding to the FMC smear array is shown in Figure 7. A constant static resolution of 100 lines/mm was assumed over the entire format, so that the degradation shown is due entirely to the FMC method. As an example, the smear array due only to roll (4.5 mr/sec) of the RPY arrays is herein presented (Figure 8). For all four smear arrays, s_x is plotted over s_y at each grid point. The x_p-axis is positive to the right, the y_p-axis, downward.

Using the relocatable binary deck (RBD) for inputting IMS002, about five cases can be computed in 1.0 min. of CDC 3600 time.

MONTE CARLO SIMULATION PROGRAM MCIMS

The random processes simulated in the current version of MCIMS include the RPY

IMC RESOLUTION (L/MM), NO V/H SENSOR ERROR. AWAR= 92.3 STATIC RESOLUTION= 100

87	87	87	87	87	87	87	87	87	87	87
90	90	89	89	89	89	89	89	89	90	90
93	92	92	92	92	91	92	92	92	92	93
95	95	95	94	94	94	94	94	95	95	95
98	98	97	97	97	97	97	97	97	98	98
99	99	100	100	100	100	100	100	100	99	99
96	96	97	97	97	97	97	97	97	96	96
93	93	94	94	94	94	94	94	94	93	93
90	91	91	91	91	91	91	91	91	91	90
88	88	89	89	89	89	89	89	89	88	88
86	86	86	86	86	87	86	85	86	86	86

FIG. 7. Resolution array.

```
IMAGE SMEAR FOR A ROLL RATE OF 4.50 MR/SEC AND 0.0040 SEC EXPOSURE
  0.1  0.1  0.0  0.0  0.0  0.0 -0.0 -0.0 -0.0 -0.1 -0.1
 11.0 11.0 11.0 11.0 11.0 11.0 11.0 11.0 11.0 11.0 11.0

  0.1  0.0  0.0  0.0  0.0  0.0 -0.0 -0.0 -0.0 -0.0 -0.1
 11.0 11.0 11.0 11.0 11.0 11.0 11.0 11.0 11.0 11.0 11.0

  0.0  0.0  0.0  0.0  0.0  0.0 -0.0 -0.0 -0.0 -0.0 -0.0
 11.0 11.0 11.0 11.0 11.0 11.0 11.0 11.0 11.0 11.0 11.0

  0.0  0.0  0.0  0.0  0.0  0.0 -0.0 -0.0 -0.0 -0.0 -0.0
 11.0 11.0 11.0 11.0 11.0 11.0 11.0 11.0 11.0 11.0 11.0

  0.0  0.0  0.0  0.0  0.0  0.0 -0.0 -0.0 -0.0 -0.0 -0.0
 11.0 11.0 11.0 11.0 11.0 11.0 11.0 11.0 11.0 11.0 11.0

  0.0  0.0  0.0  0.0  0.0  0.0  0.0  0.0 -0.0  0.0 -0.0
 11.0 11.0 11.0 11.0 11.0 11.0 11.0 11.0 11.0 11.0 11.0

 -0.0 -0.0 -0.0 -0.0 -0.0  0.0  0.0  0.0  0.0  0.0  0.0
 11.0 11.0 11.0 11.0 11.0 11.0 11.0 11.0 11.0 11.0 11.0

 -0.0 -0.0 -0.0 -0.0 -0.0  0.0  0.0  0.0  0.0  0.0  0.0
 11.0 11.0 11.0 11.0 11.0 11.0 11.0 11.0 11.0 11.0 11.0

 -0.0 -0.0 -0.0 -0.0 -0.0  0.0  0.0  0.0  0.0  0.0  0.0
 11.0 11.0 11.0 11.0 11.0 11.0 11.0 11.0 11.0 11.0 11.0

 -0.1 -0.0 -0.0 -0.0 -0.0  0.0  0.0  0.0  0.0  0.0  0.1
 11.0 11.0 11.0 11.0 11.0 11.0 11.0 11.0 11.0 11.0 11.0

 -0.1 -0.1 -0.0 -0.0 -0.0  0.0  0.0  0.0  0.0  0.1  0.1
 11.0 11.0 11.0 11.0 11.0 11.0 11.0 11.0 11.0 11.0 11.0
RMS SMEAR=11.0 MICRONS.
```

FIG. 8. Image smears due to roll.

rates, the RPY angles, and the V/H error. Generally the RPY motions and V/H errors are the most important processes. The RPY angles, which contribute to image degradation only through programming errors in the FMC system, usually have negligible effect on AWAR. However, for slow aircraft in high winds and for satellites in orbits where the earth's rotation provides a strong cross-track component, yaw may cause appreciable degradation.

At present, all seven of the random variables are generated as independent random normal deviates. The deterministic portion of MCIMS is a straight-forward modification of IMS002. For heuristic reasons, AWAR, as calculated in IMS002 for low contrast targets, again serves as the measure of system permance.

Obviously, the RPY rates and angles must actually be statistically dependent. The dearth of published experimental data on vehicle-inertial-platform stability makes it it difficult to adequately specify the variance-covariance matrix for any installation, hence the assumption of independence. On the other hand, one-sigma values, assuming normal distributions, are often available for these six random variables and can be used

TABLE II. RMS SMEAR VS. V/H ERROR

Percent V/H Error	*RMS Smear (Microns)*
−10.0	2.10
− 5.0	1.33
− 2.0	1.04
− 1.0	1.00
0.0	.99
1.0	1.02
2.0	1.08
5.0	1.41
10.0	2.19

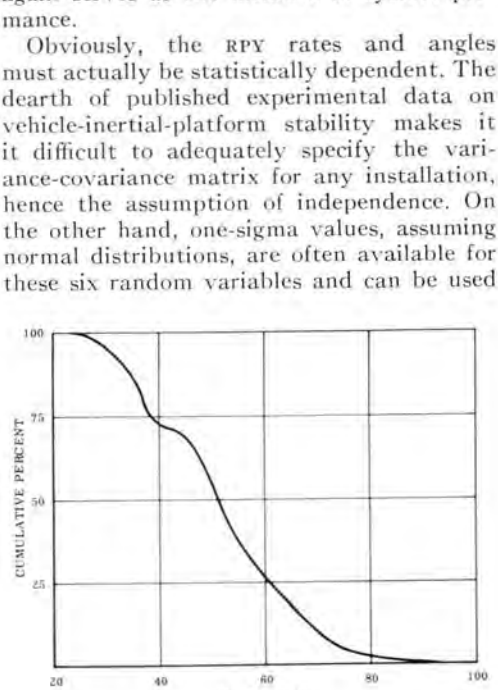

FIG. 9. Performance curve.

be used as input to MCIMS. Zero means are assumed only for the RPY rates.

Figure 9 shows a typical performance curve obtained with MCIMS. The camera data are the same as those used for the other figures of this paper. Static resolution was again taken to be 100 lines/mm. One-sigma RPY rates of 4.5, 2.5, and 1.5mr/sec, respectively, and a V/H error of 2.0 per cent were assumed. The curve shows that 50 per cent of all photographs taken under the stated conditions should have AWAR's, computed as 121-point averages, in excess of 50 lines/mm.

References

Hallert, Bertil, *Photogrammetry*, McGraw-Hill, New York, 1960.

Kawachi, D., Image Motion and Its Compensation for the Oblique Frame Camera, PHOTOGRAMMETRIC ENGINEERING, v. 31, no. 1, 1965a, pp. 154–165.

Kawachi, D., Image Motion Due to Camera Rotation, PHOTOGRAMMETRIC ENGINEERING, v. 31, no. 5, 1965b, pp. 861–867.

Manual of Photogrammetry, vol. 1, 3rd edition, 1966.

Perkins, C. D., and Hage, R. E., *Airplane Performance Stability and Control*, John Wiley & Sons, Inc., New York, 1949.

(*Continued from page 1151*)

Detección de Árboles Enfermos

Por *Prof. Merle P. Meyer*, y *Prof. David W. French*

Los programas de control más eficaces para la enfermedad del olmo holandés, marchitamiento del roble, y otras enfermedades de los árboles, necesitan un sistema de detección que sea más rápido, menos costoso y tan digno de confianza como la inspección terrestre. Varias áreas en Minnesota fueron fotografiadas utilizando la película Kodak Ektachrome Infrarroja (color falso) dentro de un radio de elevaciones de vuelo, con cubrimiento estereoscópico y sin él, y durante diferentes épocas del año. Las comparaciones de los resultados de las interpretaciones fotográficas, con las observaciones en el terreno, indican que existen problemas de aplicación, pero al mismo tiempo sugieren que esta técnica puede servir como un medio práctico de detección de enfermedades.

PHOTO. ENGR., SEPTIEMBRE 1967, PÁGINA 1035

Ajuste de Bloques por Transformaciones Polinómicas*

Por *G. H. Schut*

Esta publicación contiene la descripción de un programa FORTRAN IV para el ajuste de fajas independientes y de bloques de fajas por medio de transformaciones polinómicas.

En julio de 1965 la computadora IBM 1620 de los laboratorios de la NRC, fue reemplazada por un sistema IBM 360. Se hizo evidente que eventualmente los actuales programas de ajuste de fajas y bloques polinómicos, escritos en el lenguaje simbólico SPS para la IBM 1620 (1, 2, 3) tendrían que ser reemplazados por un programa FORTRAN para el modelo IBM S/360.

Antes de que esto se hiciera, se llevó a cabo una investigación para determinar si al mismo tiempo, las transformaciones polinómicas de fajas deberían reemplazarse por una transformación lineal de modelos. Esta investigación demostró (4) que con la baja densidad del control terrestre—lo cual es normal en levantamientos topográficos—la transformación polinómica de fajas da por lo menos, resultados tan precisos como los de la transformación lineal de modelos. Esto se lleva a efecto a un costo mucho menor y con requisitos más simples en el manejo de la información.

En consecuencia, se determinó que valía la pena programar nuevamente el ajuste polinómico en lenguaje FORTRAN.

El programa FORTRAN sirve igualmente para el ajuste de fajas y para el ajuste de bloques.

Las fórmulas de transformación se han simplificado hasta cierto punto. Estas simplificaciones tienen un efecto mínimo sobre los resultados.

PHOTO. ENGR., SEPTIEMBRE 1967, PÁGINA 1042

* *Nota:* Traducido por la Sección de Traducciones de la Escuela Cartográfica del Servicio Geodésico Interamericano (IAGS).